Temperatures of Air Parcels Lifted from the Surface: Background, Application and Nomograms

FREDERICK SANDERS

Marblehead MA 01945

(Manuscript received 23 July 1986, in final form 17 September 1986)

ABSTRACT

When the temperature of a parcel lifted adiabatically from the surface to a given pressure level (SLT) is subtracted from the ambient temperature at that level, the result is the surface lifted index (SLI) for that level. This quantity, for the 500-mb pressure level, has been found useful in the very-short-range prediction of deep and often severe convection. We examine the thermodynamics of the lifting process, finding that the SLTs are sensitive mainly to surface dewpoint for very warm humid air and to surface temperature for cold air.

Nomograms are presented for determination of SLT's for 850, 700 and 500 mb, given surface temperature and dewpoint and a nominal surface pressure of 950 mb. An approximate correction is given for departures from this pressure. These are intended for use with the routine aviation surface observations. An additional nomogram is provided for use over the sea.

An example of application is shown, based on hourly surface observations and on ambient temperatures interpolated between standard rawinsonde analysis times. Severe convection is observed where large parcel buoyancy is indicated by SLI at 500 mb, with no negative buoyancy at 700 or 850 mb. Apparently unreliable measurements of dewpoint in warm humid air constitute a significant analysis problem, and reliable large-scale predictions of ambient temperature are a requirement for optimum real-time use.

1. Introduction

Measures of the susceptibility of the atmosphere to cumulus convection are primary ingredients in the methodology of prediction of shower and thunderstorm activity. Examples which have been widely used for a long time are the Showalter (1953) Stability Index (SSI) and the Lifted Index (LI) introduced by Galway (1956). Both imply the conceptual simulation of a trial cumulus cloud, composed in the former case of air originating at the 850-mb level and in the latter of air representing an average of the potential temperature and mixing ratio in the 100-mb layer nearest the ground. Both imply no mixing of environmental air into the cumulus updraft above cloud base. Both represent the buoyant available energy by comparing the temperature of the hypothetical cloud parcel lifted adiabatically to 500 mb, saturated or not as appropriate, with the ambient temperature at that level.

Leaving aside for the moment the possibility of their prediction, the SLI and LI require rawinsonde observations for their evaluation. These are available in general only at 1200 GMT and 0000 GMT, not particularly desirable times in the strong diurnal cycle of heating and cooling over land, since they correspond to 0700 and 1900 LST in the Eastern Time Zone and to 0400 and 1600 LST in the Western Time Zone. A measure of buoyant instability taken at 1000–1200 LST, just prior to the usual time of onset of convection, would be highly valuable as would be the ability to monitor the continuing supply of unstable air to ongoing convective systems during the afternoon and evening. Furthermore, rawinsonde locations are typically a few hundred kilometers apart. Within these distances, narrow tongues of maximum instability can often go undetected.

Realizing these limitations inherent in a wholly rawinsonde-based measure, Means (1952) suggested calculation of a stability index based on surface observations of temperature and dewpoint, since these are available in the United States once an hour from a network of stations about 100 km apart. Of course, the 500-mb ambient temperature must be specified; Means (1952) suggested interpolation in space and constancy in time, derived from the latest 500-mb analysis. This "surface lifted index" (SLI) was evidently used in the Chicago area for some time, but we are not aware of any systematic evaluation of its effectiveness. Means (1952) mentions only that from study of several situations, a necessary although not sufficient condition for tornadoes appeared to be an SLI-value of −4 or lower, denoting that the surface lifted temperature (SLT) was at least 4°C warmer than the ambient air at 500 mb.

Strictly speaking, any of the indices requires a forecast of the ambient 500-mb temperature. For the short time ranges involved in forecasting of convection, operational numerical models can probably provide a

value at least as accurate as persistence or simple extrapolation.

In most cases the more challenging problem is to predict the temperature and humidity of the air rising in the convective clouds. First, there is the difficulty in dealing with the mixing of environmental air into the updraft. We will sidestep this issue by concentrating on the most vigorous cumulus clouds in the ensemble, and by noting that these may often contain updrafts composed of undilute air from near the ground (Barnes, 1970; Drogemeier and Wilhelmson, 1985). The importance of relatively deep moisture in the ambient atmosphere was recently emphasized by Mostek et al. (1986) in an application of satellite soundings. The value of these soundings, however, was found to be enhanced by consideration of surface observations in their interpretation. Comparison of their Figs. 5 and 17, moreover, suggests that in the case discussed the surface observations themselves may have been approximately as informative as the soundings so far as convection was concerned.

In any event, a major challenge is the great spatial variability, over land, in the diurnal charging of the surface boundary layer in the morning and its subsequent evolution during the day and evening. This variability is not now well predicted, so that monitoring it, e.g., by calculation of SLT from observations, becomes of the greatest importance.

Given pressure at the station level as well as surface temperature and dewpoint, automated calculation of SLT is simple and useful, as demonstrated by Hales and Doswell (1982). This value, compared with an ambient value determined by extrapolating the 500-mb isotherms in the geostrophic flow, yields a graphical product which is displayed at the National Severe Storms Forecast Center (NSSFC) as part of the Centralized Storm Information System (CSIS) and is used in severe thunderstorm forecasting. Comparable capability no doubt exists in a number of other organizations.

The above notwithstanding, there may be interest in having a graphical method for rapid determination of SLT. For one reason or another the automated product may not be available for the desired area. Observations from a new station, or any observation of opportunity such as from a ship, will likely not be processed by the system but can be handled with a simple nomogram. Sensitivity to increments of (or errors in) temperature or dewpoint can be quickly and easily assessed. This paper presents such a device.

2. Background

A portion of a Skew T–log P diagram appears in Fig. 1 with a number of sample evaluations of SLT. These are arranged in two sets, representative broadly 1) of the most warm and humid conditions likely to be encountered in the United States, and 2) of the coldest air mass in which the possibility of deep convection is likely to be considered.

In the former group we consider surface temperatures (at 1000 mb) to be 30° or 32°C with dewpoints of 25° or 27°C. Lifting condensation levels (LCLs) range from about 960 to 905 mb. Values of SLT at 500 mb, denoted SLT(500), lie between about 1.5° and 4°C. Note that a 2°C increment in surface temperature with dewpoint held constant affects SLT(500) by less than 1°C. On the other hand, a change of 2°C in dew-

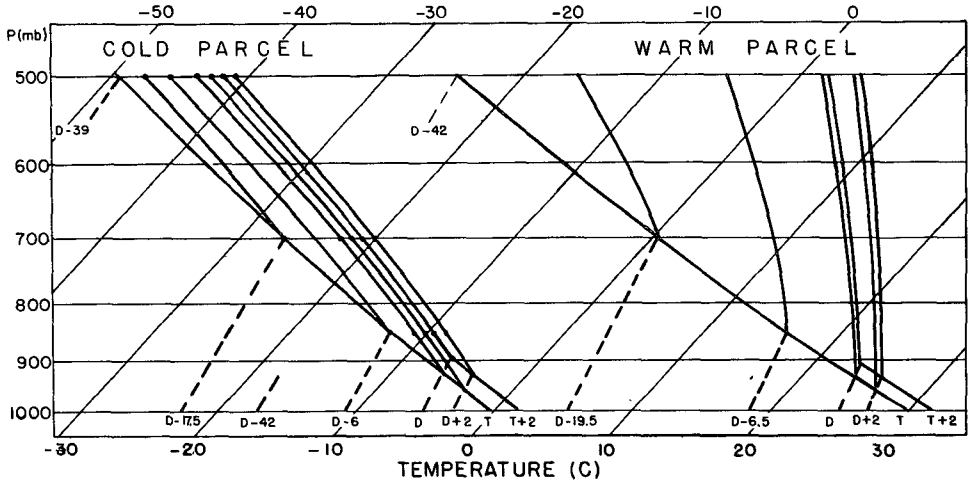

FIG. 1. Portion of a Skew T–Log$P$ diagram, illustrating the process of determining the surface lifted temperature, and the sensitivity of the result to perturbations of surface temperature, T, and dewpoint, D, for typical cold and warm parcels. Less steeply sloping heavy lines are dry adiabats; more nearly vertical ones are saturation adiabats. Dashed lines are isopleths of mixing ratio. These isopleths for large dewpoint perturbations, broken in some cases, are to illustrate conditions for which the lifting condensation level is just 850, 700 or 500 mb.

point with temperature held constant produces a change of almost exactly 2°C in SLT(500). For these warm, humid conditions, the lifted temperature can be regarded as more sensitive to change of dewpoint than to change of temperature. If the lifting is carried out only to 700 or 850 mb, say, for assessment of the presence and effectiveness of a "lid" (Carlson et al., 1983) in preventing surface air from reaching its level of free convection (LFC), then similar characteristics are found, except that the sensitivity to dewpoint is not quite so large at the lower levels.

In the latter, colder group of sample conditions, we consider surface temperatures of 0° or 2°C with dewpoints of −5° or −3°C. With the same dewpoint depression as before, LCLs occur at pressures about 5 mb lower. The sensitivities to increments of surface temperature and dewpoint are qualitatively reversed. That is, an increase of 2°C in temperature raises SLT(500) by more than 1.5°C, while the same increase in dewpoint produces a rise of less than 1°C.

These differences in behavior are due, of course, to the effects of latent heating. In the absence of this heating, the change in SLT would be given by the differentiated form of Poisson's equation,

$$\delta T = \delta\theta(500/1000)^{R/c_p} = 0.82,$$

where R is the gas constant for dry air (286 $m^2\ s^{-2}\ K^{-1}$) and c_p is the specific heat of air at constant pressure (1000 $m^2\ s^{-2}\ K^{-1}$). Here T can be identified with SLT(500) and θ with surface temperature. In this case an increase of 2°C in surface temperature would produce a 1.64°C rise in SLT(500).

When latent heating occurs, we consider the equivalent-potential temperature, which can be expressed by

$$\theta_e = \theta \exp(Lq/c_pT_c),$$

where L is the latent heat of condensation of water vapor ($2.5 \times 10^6\ m^2\ s^{-2}$), q its mixing ratio, and T_c the temperature at which condensation (or evaporation) occurs. Differentiating this expression logarithmically at constant pressure, we have,

$$\delta \ln\theta_e = \delta \ln T + (L/c_pT_c)\delta q. \quad (1)$$

If at 1000 mb we keep the dewpoint the same and increase the temperature, then the increase in θ_e is given by

$$\theta_e^{-1}(1000)\delta\theta_e(1000) = T^{-1}(1000)\delta T(1000).$$

During adiabatic ascent to 500 mb, the value of θ_e is conserved, for both the original air parcel and the warmed parcel. So $\theta_e(500) = \theta_e(1000)$ in both instances and

$$\theta_e^{-1}(500)\delta\theta_e(500) = \theta_e^{-1}(1000)\delta\theta_e(1000) = T^{-1}(1000)\delta T(1000).$$

Therefore, (1) at 500 mb can be written

$$T^{-1}(500)\delta T(500) + (L/c_pT_c)\delta q_s(500) = T^{-1}(1000)\delta T(1000), \quad (2)$$

where we have assumed that the air is saturated at this level in both instances and $q_s(500)$ is its mixing ratio. The temperature increase at 1000 mb is reflected at 500 mb partly as a temperature rise and partly as an increase in the saturation mixing ratio.

Now the change in saturation mixing ratio with temperature at constant pressure is given by a form of the Clausius-Clapeyron equation,

$$q_s^{-1}\delta q_s = (L/R_vT_c)T^{-1}\delta T, \quad (3)$$

or, at 500 mb,

$$\delta q_s(500) = [L/R_vT^2(500)]q_s(500)\delta T(500). \quad (4)$$

Here R_v is the gas constant for water vapor (461 $m^2\ s^{-2}\ K^{-1}$). Substituting (4) into (2), we find

$$\delta T(500) = \left[\frac{T(500)/T(1000)}{(1 \times L^2q_s(500)/R_vc_pT)}\right]\delta T(1000). \quad (5)$$

Next we consider what happens when the 1000-mb temperature is held constant while the dewpoint is increased. In this case, we find from (1) that

$$\delta \ln\theta_e(1000) = (L/c_pT_c)\delta q_s(1000), \quad (6)$$

while the change in $q_s(1000)$ with $T_d(1000)$, the dewpoint temperature, is obtained from (3) as

$$\delta q_s(1000) = [Lq_s(1000)/R_vT(1000)]T_d^{-1}(1000)\delta T_d(1000). \quad (7)$$

Substitution from (6) and (7) into (1) then leads to

$$T(500) = \frac{[T(500)/T_d(1000)][L^2q_s(1000)/R_vc_p]}{[1 + L^2q_s(500)/R_vc_pT^2(500)]}\delta T_d(1000). \quad (8)$$

For the examples illustrated in Fig. 1, we can now use (1), (3), (5) and (8), together with the thermodynamic diagram to determine the saturation adiabats, to examine how the alterations of temperature and dewpoint at 1000 mb influence the resulting temperature and saturation mixing ratio at 500 mb. Results are shown in Table 1.

We see in comparing results for the cold and warm parcels that the proportional change in $\theta_e(1000)$ produced by the temperature increase for the latter is only slightly smaller than for the former. At the higher temperature, however, owing to the great sensitivity of q_s to T, the proportional change produced by the increase in dewpoint is about six times larger than for the cold parcel. The dewpoint change produces about half the increase in θ_e resulting from the temperature change

TABLE 1. Thermodynamic calculations for sample parcels.

Level (mb)	Cold air			Warm air		
	T (K)	D (K)	q (10^{-3})	T (K)	D (K)	q (10^{-3})
1000	273	268	2.65	303	298	20.2
500	230	230	0.16	274.5	274.5	9.6

	$T+2, D$	$T, D+2$	$T+2, D$	$T, D+2$
$T(1000)$ [K]	2	0	2	0
$q_s(1000)$ [$\times 10^{-3}$]	0	0.40	0	0.24
$\ln\theta_e(1000)$	0.0073	0.0037	0.0066	0.0219
$T(500)$ [K]	1.61	0.79	0.66	2.02
$q_s(500)$[$\times 10^{-3}$]	0.02	0.035	0.45	1.6
$\ln T(500)$	0.0070	0.0034	0.0024	0.0073
$[L/(c_pT_c)]q_s(500)$	0.0002	0.0004	0.0041	0.0145

in the cold air, but about three times this increase in the case of the warm air.

These same changes in θ_e at 500 mb, however, are differently distributed between effects on T and on q_s. For the cold parcel, the effect of raising the surface temperature is almost entirely on raising the temperature at 500 mb, with little effect from raising saturation mixing ratio. Hence the result is close to that for a dry-adiabatic process. Even when the surface dewpoint is increased, the preponderant effect is on temperature increase at 500 mb. For the warm air, however, the preponderant effect, by a factor of almost 2, is in raising $q_s(500)$, whether the surface temperature or the surface dewpoint is increased. In the latter instance, the resulting increase in $T(500)$ is nevertheless substantial, because of the very large increase in θ_e.

As noted by Means (1952), Showalter had suggested that the wet-bulb potential temperature be denoted according to its value at 500 mb, rather than the customary 1000 mb, implying that it could then be identified with SLT(500) and used for assessment of stability. This identification is valid only if the air is saturated upon reaching the 500-mb level. As can be seen in Fig. 1, saturation is reached if the 1000-mb dewpoint depression is no larger than 39°C for the cold-air sample or 42°C for the warm one. Since such large depressions are seldom observed, we can assume that SLT(500) represents saturated air for practical purposes, and thus can be regarded as a wet-bulb potential (or equivalent potential) temperature, reduced to 500 mb. This identification cannot readily be made, however, for SLT(700) or SLT(850), since inspection of Fig. 1 shows critical dewpoint depressions that are within the range of common observation, especially at 850 mb. If an air parcel is not yet saturated upon arriving at the specified pressure level, of course, the surface dewpoint has no effect upon the SLT (at the level of thermodynamic precision herein employed). In this instance, the SLT is in effect a potential temperature.

In all the foregoing we have assumed a surface pressure of 1000 mb. In practice, surface pressures will range widely over land, principally on account of station elevation. An idea of the effect of station pressure on SLT is offered in Fig. 2. Since θ and q_s are both larger at the surface as lower station pressures are considered, SLT increases with station elevation. This effect varies substantially with surface temperature and with the pressure level for which SLT is desired, but it varies little with station pressure (hence elevation). The station-pressure increment required to produce a 1°C change in SLT varies from 12 mb for the cold-air parcel at about 750 mb, with the lifted level at 500 mb, to 25 mb for the warm-air parcel at 850 mb station pressure but lifted to 700 mb.

3. The nomograms

The results, in effect, of a large number of operations of the type illustrated in Fig. 1 appear in Figs. 3–6. The first three of these are designed for use with hourly surface-aviation (SA) observations over the United States. Hence the ordinate and abscissa are labeled in °F (32° + 0.545°C) for utility. The range of temperature is believed to cover all situations in which deep convection might be remotely considered. The range of dewpoints extends into drier conditions than probably necessary. The last of the nomograms is designed for use over the sea, where the surface air is not excessively dry. The coordinates here are labeled in °C for ease of use with the usual plotting practice. Regions where the isopleths of SLT run horizontally correspond to unsaturated conditions at the reference pressure level, where the result is independent of surface dewpoint, as noted previously. In the saturated regions, note that the isopleths are relatively vertical in the upper-right portions and relatively horizontal in the lower left. This contrast shows the differing sensitivity of SLT

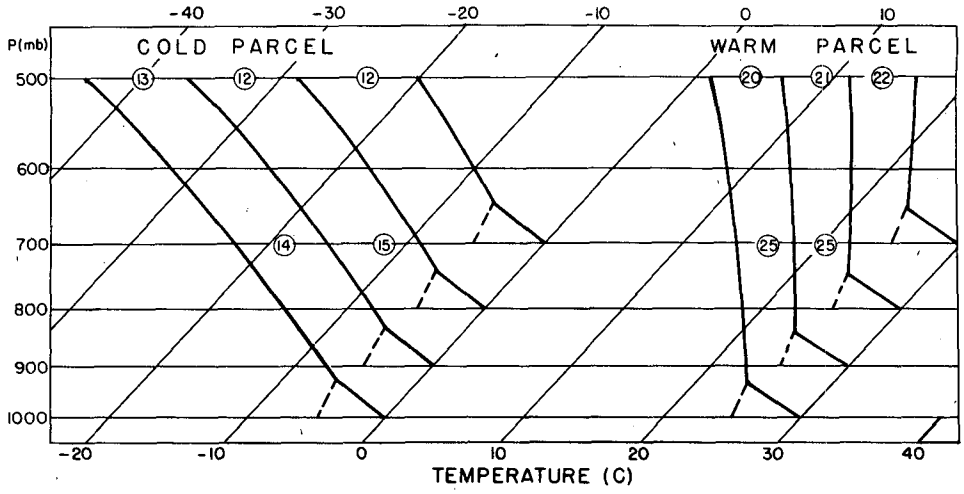

FIG. 2. As in Fig. 1 but illustrating the effect of variability of station pressure. Circled numbers represent station-pressure increments required to change SLT by 1°C, placed at the level to which the parcel is to be lifted.

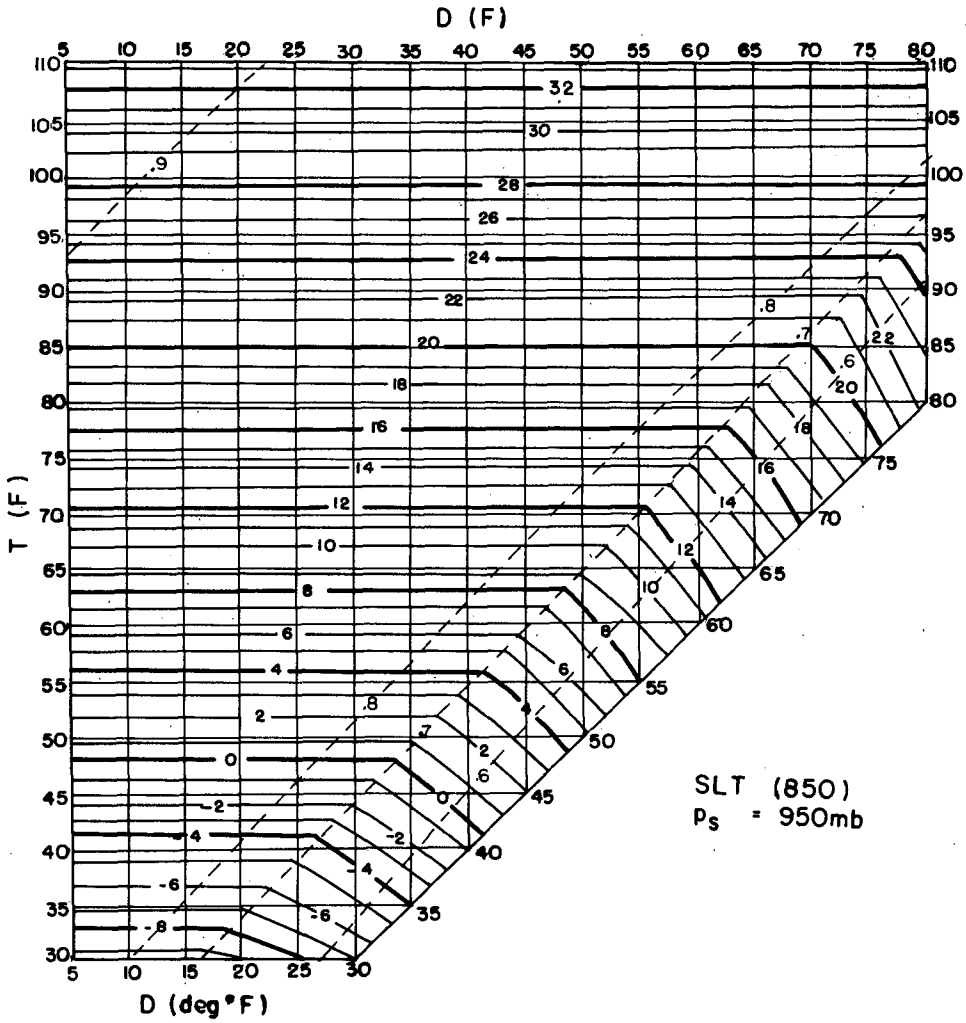

FIG. 3. Nomogram for SLT(850) (C), given T and D (F), for station pressure 950 mb. Thin dashed lines indicate the increment of SLT for a change of 10 mb in station pressure.

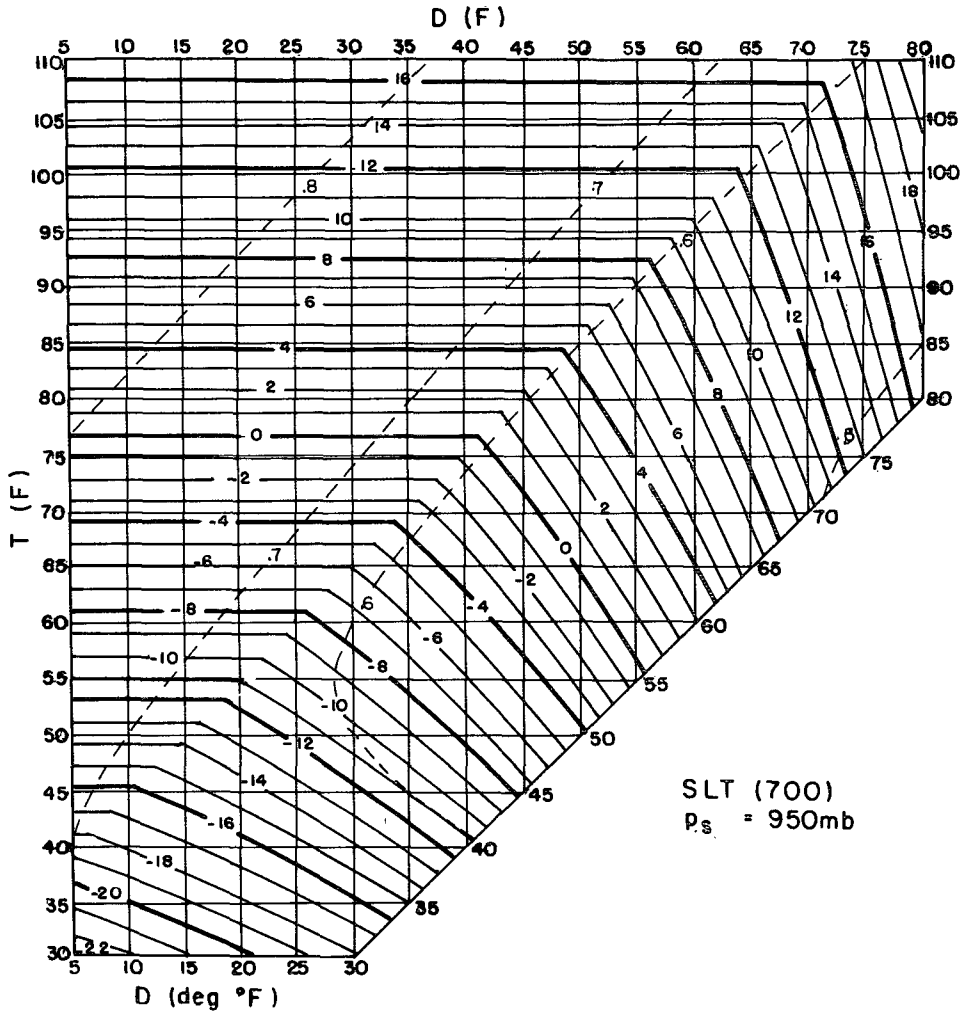

FIG. 4. As in Fig. 3 but for SLT(700).

to surface temperature and dewpoint, as discussed above.

The nomograms for use over land are valid for surface pressures of 950 mb, corresponding to an elevation of about 550 m, as a Standard Atmosphere average. Allowing, for simplicity, a rate of change of SLT(500) with station pressure of 1°C (15 mb)$^{-1}$, and assuming Standard Atmosphere conditions, then the elevation of each station would yield a correction to the SLT(500) read from Fig. 6. These corrections are mapped in Fig. 7. The zero-line runs through the Central Plains, a convectively active region. Corrections at stations in the Rocky Mountains are as high as +10°–15°C, while at stations near sea level the correction is −4°C. In the Rockies greater accuracy would be achieved with a nomogram based on a more realistic station pressure. Further, the corrections are not accurate when the temperatures and dewpoints are exceptionally high or low and when the reference level to which the parcel is lifted is different from 500 mb. Suitable values could, of course, be obtained.

4. An example

The detail in the estimated stability field which can be obtained by use of SLTs calculated from the aviation surface network, and how closely this detail is related to deep convection, is illustrated by the situation on the afternoon of 11 May 1985. A number of severe-thunderstorm events were reported in the central United States, as shown in Fig. 8. Close inspection indicates that almost all fell in one of three clusters: 1) a swath originating along the Kansas–Missouri border northward into western Iowa at about 2000 GMT (2 pm CST) and moving northeastward to Minnesota and Wisconsin 5 h later; 2) a highly concentrated group

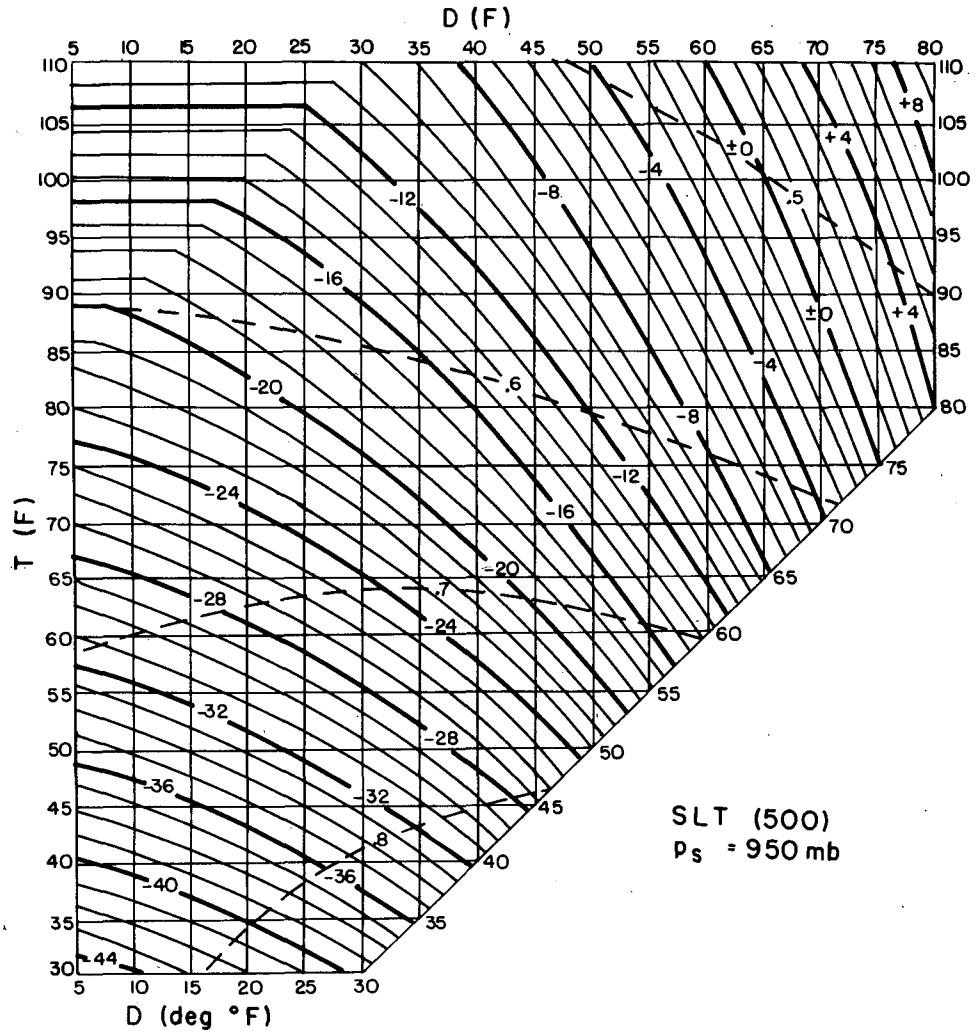

FIG. 5. As in Fig. 3 but for SLT(500).

first detected in northeastern Nebraska at about 2100 GMT (3 pm CST) thence moving to eastern South Dakota by 7 pm CST; and 3) a small group in northeastern Texas, 3–5 pm CST. All three clusters contained tornadoes, but only weak ones, and damage was relatively modest.

The sea level pressure patterns and surface winds for 1800 and 2100 GMT (noon and 3 pm CST) are displayed in Figs. 9–10. A deep low center moved northeastward in eastern South Dakota. A high evidently lay in the southeastern states, beyond the edge of the map. The shape of the isobars south and southeast of the low suggested confluence. Indeed, the winds indicated a line of confluence between southerlies from the Gulf of Mexico and southwesterlies with a history of recent descent from the Rocky Mountains along the western edge of the map. This dry-line advanced noticeably during the 3-h period in Texas and along the Kansas–Missouri and Nebraska–Iowa borders, but not elsewhere.

Selected observations of thunderstorm activity and of deep cumulus clouds are plotted on Figs. 9a and 10a, along with transcribed outlines of the VIP-3 (>41 dBZ) and VIP-5 (>50 dBZ) reflectivity contours from radar composite maps received on facsimile. At the earlier time, no VIP-5 echoes were reported, but a fragmented line of VIP-3 echoes from northeastern Texas to northeastern Missouri, accompanied by a number of reports of thunder, represented the remains of an earlier convective system. It lay definitely east of the major confluence line but was associated with a turning of winds to the southwest across part of Arkansas (Fig. 9b).

Nearly along the major line were numerous reports of towering cumulus and cumulonimbus from central Texas into Oklahoma, confirmed by satellite imagery

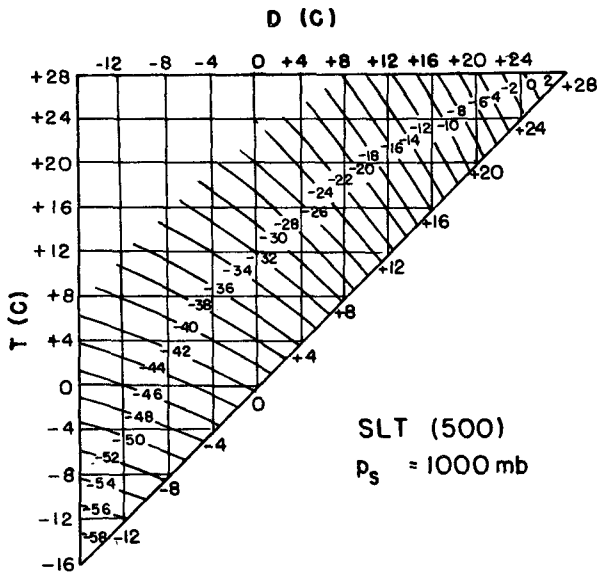

FIG. 6. As in Fig. 5 but with T and D (°C) as coordinates, and for surface pressure 1000 mb.

(not shown) and displaying one small, new, VIP-3 echo. Elsewhere were less well-organized areas of large cumulus and echoes, in the south and east quadrants of the surface low and over the eastern edge of the map from the Gulf of Mexico to the Great Lakes.

At the later time (3–4 pm CST), substantial changes had occurred, except on the eastern edge. The old convective area east of the confluence line had nearly, but not quite, dissipated. The convection along the line in Texas had strengthened slightly and was about to produce some severe events (cf. Fig. 8). The convection associated with the low center itself had strengthened markedly, with substantial areas of VIP-5 echo and numerous reports of cumulonimbus and thunder. The convective system extending from Nebraska into southeastern South Dakota was beginning (Fig. 8) to produce tornadoes.

The most dramatic development, however, was the sudden appearance of a new line segment of intense (VIP-5) echo, from northern Missouri to central Iowa. Although this feature was now distinctly east of the advancing confluence line, its origin was almost exactly

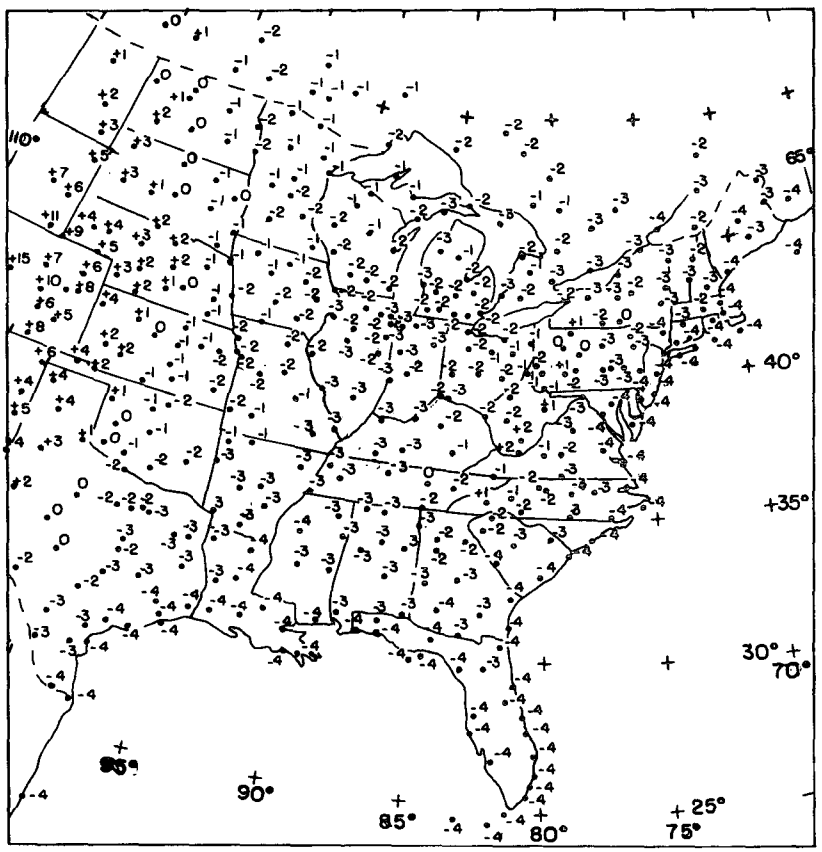

FIG. 7. Approximate adjustment in SLT(500) (°C) to value obtained from Fig. 5, for most hourly reporting stations in central and eastern United States and adjacent portions of Canada.

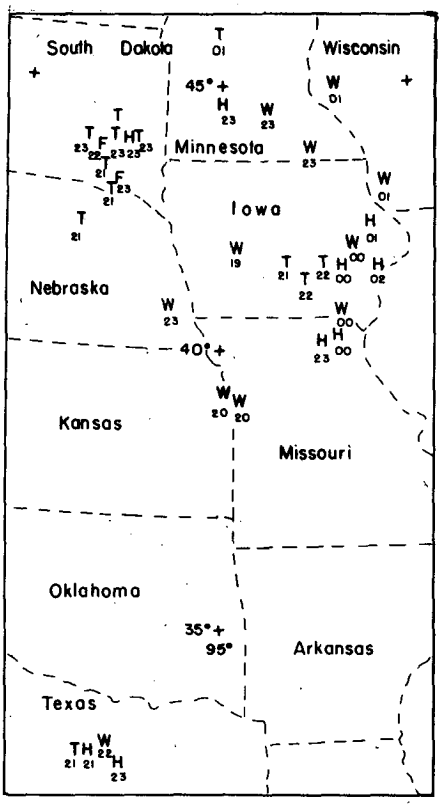

FIG. 8. Severe convective events reported in *Storm Data* (U.S. Dept. of Commerce, 1985) on 11–12 May 1985. Tornado is denoted by "T", large hail by "H", wind damage by "W" and flooding by "F". Time below each event is the nearest hour, from 1900 GMT on the 11th to 0100 GMT on the 12th. Locations of states mentioned in text are shown.

along the line in extreme eastern Kansas, as suggested in the satellite imagery at 1730 GMT (not shown) and in the radar and visual observations a short time later. (This development was not unanticipated, because it formed almost exactly along the upwind edge of a tornado watch area issued by NSSFC, prior to any indication in the cloud field.) This convective system was responsible for the first swath of severe events described above.

Series of analyses of SLT for 1800 and 2100 GMT are presented in Figs. 11 and 12, respectively. These are based on about 285 observations at each time, with results obtained by computer rather than by the nomograms displayed above. (Our experience with the nomograms indicates that a map for this area can be prepared by two persons in about 20 minutes. For the three levels shown here, the manual operation could barely keep up with the hourly observations. As a practical matter, however, one would not prepare an analysis every hour, and some skill would be quickly acquired in determining and ignoring broad regions of little interest. Nevertheless, we must admit that the advantages of automation, if it is available, are considerable.)

Patterns of SLT(850), Figs. 11a and 12a, show a broad region between 16° and 12°C in the central and eastern portions of the map. Warmer potential temperatures were found westward to the slopes of the Rockies (note that the SLTs represented unsaturated conditions), except in the northwestern corner of the map, where colder, more humid air intruded. Colder air also lay northeast of the Great Lakes, with extensions over the Lakes themselves. A weak ridge with SLT(850) > 16°C followed the confluence line between southerlies and southwesterlies at 1800 GMT. By 2100 GMT, however, it had lost its identity owing to further afternoon heating in the Western Plains and the irregular cooling produced by the convection in Nebraska and Iowa.

In the eastern and northern halves of the map, the patterns of SLT(700) seen in Figs. 11b and 12b resembled those of (SLT) and changed little during the 3-h period. The westward increase of SLT(850) in the southwestern portion, however, vanished. Evidently the higher potential temperature in the dry surface air of the Plains approximately compensated for the higher mixing ratio in the air farther east, so far as SLT(700) is concerned. A distinct contrast, due to the humidity difference across the confluence line, began to appear from northern Texas northward except where distorted by thunderstorm activity in Iowa and Nebraska, as shown by the 4°- and 8°C-isotherms.

This contrast was enhanced in the field of SLT(500), shown in Figs. 11c and 12c. The ubiquity of saturated values means that these fields also represent the surface wet-bulb or equivalent potential temperature distribution, as pointed out above. Differences in moisture were responsible for the decrease in SLT(500) from near −4°C in the moist air east of the confluence line to values as low as −16°C in the drier air to the west. The development of intense convection along such a confluence line has long been recognized as typical (e.g., U.S. Weather Bureau, 1963).

A cold spot for all three levels of lift was seen in northeast Texas at 1800 GMT (Fig. 11). It was attributable to the presence of cool air brought to the surface by preceding thunderstorm activity and had been removed, evidently by solar heating, 3 h later (Fig. 12) despite renewed convection in the region (Fig. 10a). The use of SLT for the detection of pools of air produced by thunderstorm downdrafts is similar to the use of the related moist static energy recommended by Darkow and Livingston (1975).

The SLTs, of course, refer to the temperatures of the surface parcels lifted hypothetically to the specified pressure levels. To evaluate the SLIs, as discussed earlier, it is necessary to estimate the ambient temperature fields at these levels. In the present case, this was done by analyzing the temperature fields at these levels,

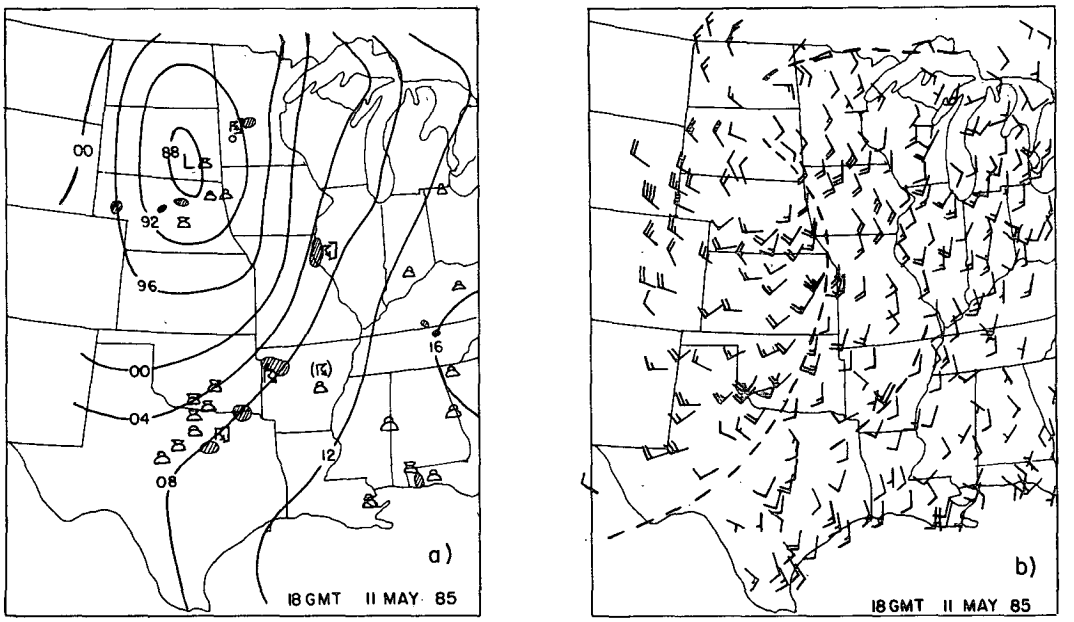

FIG. 9. For 1800 GMT 11 May 1985: (a) isobars of sea level pressure at intervals of 4 mb, labels indicating the tens and units digits, with plotted observations of towering cumulus, cumulonimbus or thunder (in conventional synoptic format), at estimated location reported; (b) plotted surface winds, with prominent wind shifts denoted by heavy dashed lines. Hatched areas in (a) denote VIP-3 echo contours in the 1735 GMT Radar Summary Chart.

without smoothing, at 1200 GMT 11 May and 0000 GMT 12 May. Thermal troughs, ridges and other features were then interpolated in position and amplitude to the times of Figs. 11 and 12. This process usually but not always yielded a result close to what would have been obtained by the simpler process of linear

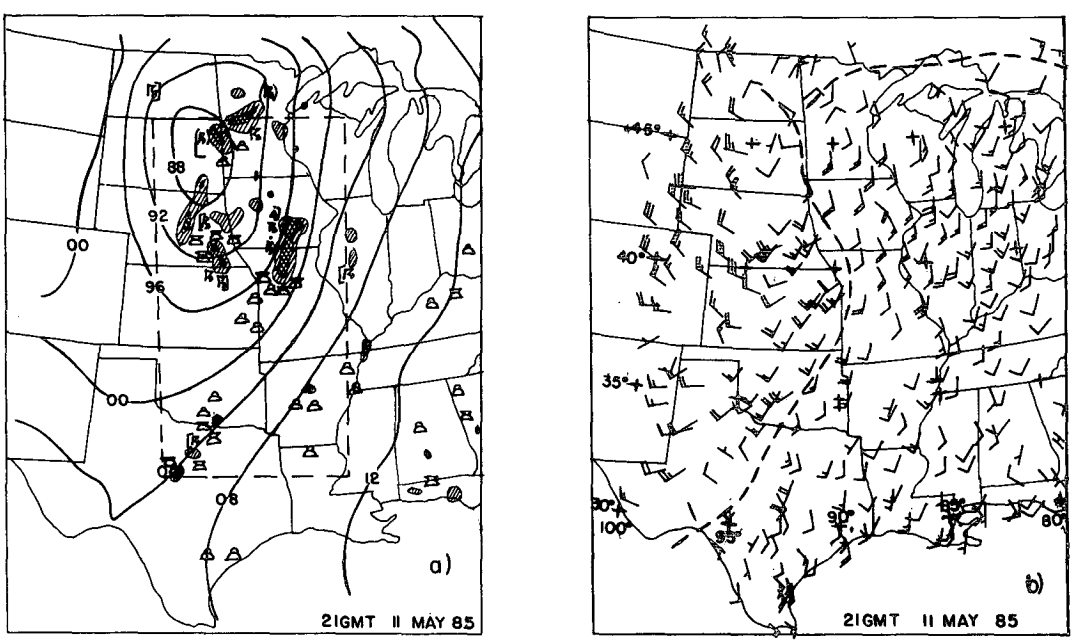

FIG. 10. As in Fig. 9 but for 2100 GMT with representation of VIP-3 and VIP-5 echo contours from 2135 GMT Radar Summary Chart.

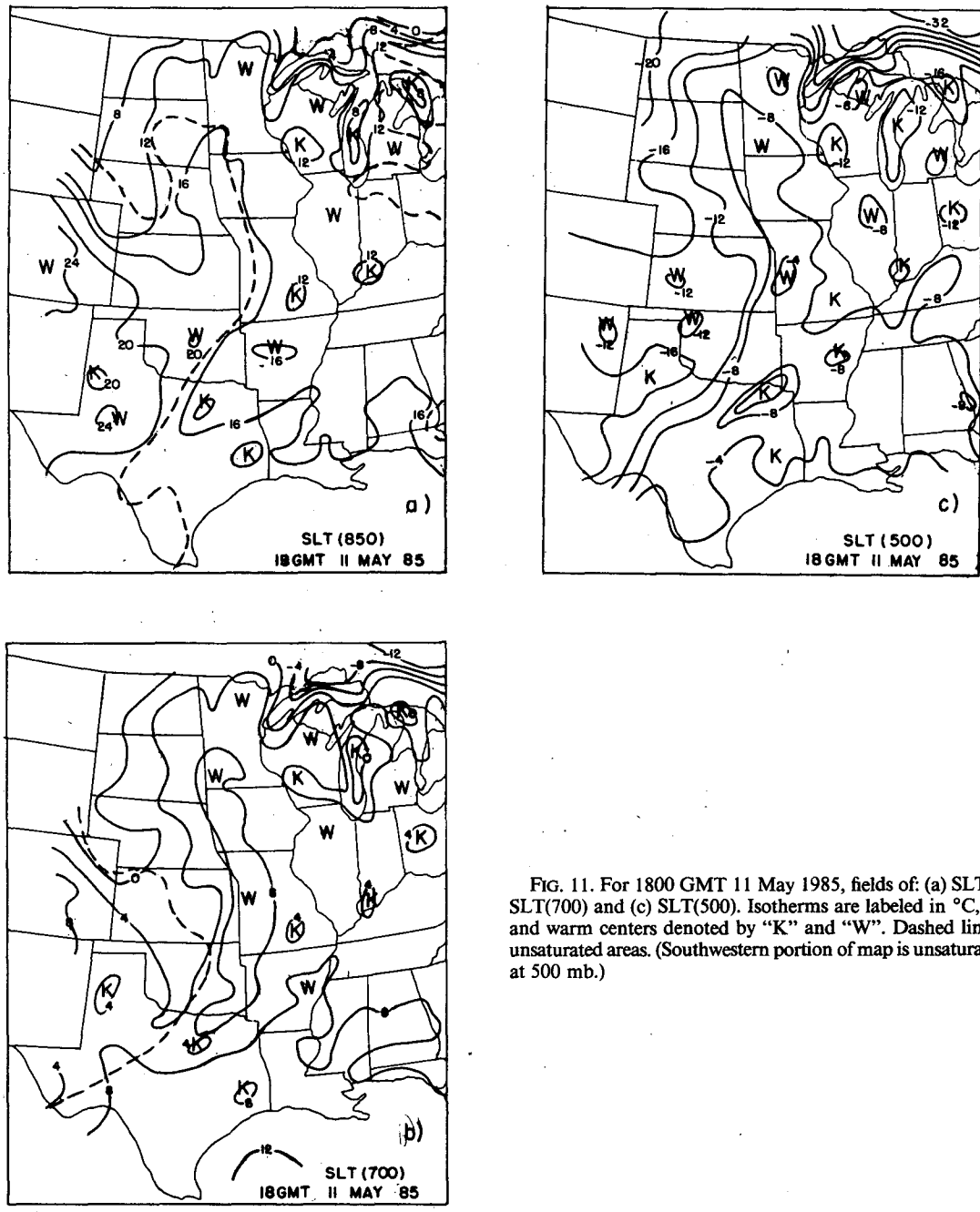

FIG. 11. For 1800 GMT 11 May 1985, fields of: (a) SLT(850), (b) SLT(700) and (c) SLT(500). Isotherms are labeled in °C, with cold and warm centers denoted by "K" and "W". Dashed lines outline unsaturated areas. (Southwestern portion of map is unsaturated except at 500 mb.)

interpolation in time, locally at the rawinsonde locations or any other grid of points. The motion of coherent ridges and troughs across the map during the 12-h period made the additional effort seem desirable. The resulting ambient patterns, and the fields of SLI obtained by comparison with Figs. 11 and 12, appear in Figs. 13 and 14. The former also contain mean observed winds, obtained by vector averaging of the observations at the beginning and end of the 12-h period.

A meridionally oriented thermal ridge moved eastward across the central or eastern part of the map at all levels. At 850 mb this continued as a distinct ridge into western Texas, roughly coincident with a belt of maximum west-southwesterly winds. At 500 mb this pattern was interrupted by a trough of cold air extending southwestward from Missouri into northeastern Texas, evidently associated with the earlier convective system there. Most significantly, a narrow zonal trough

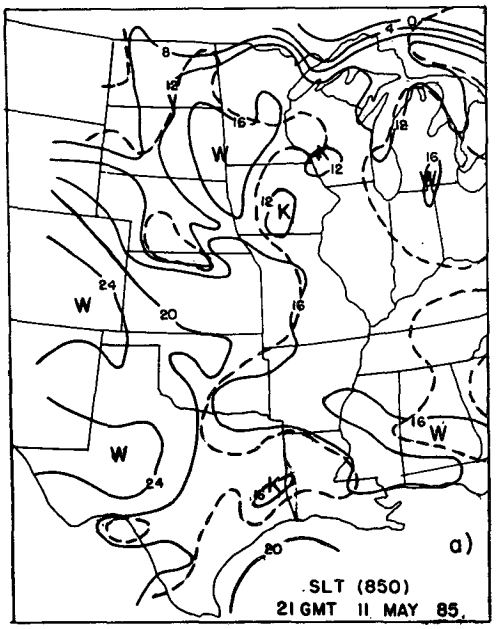

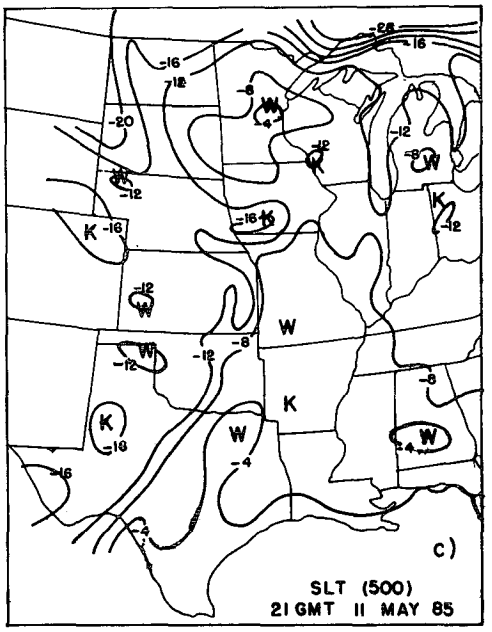

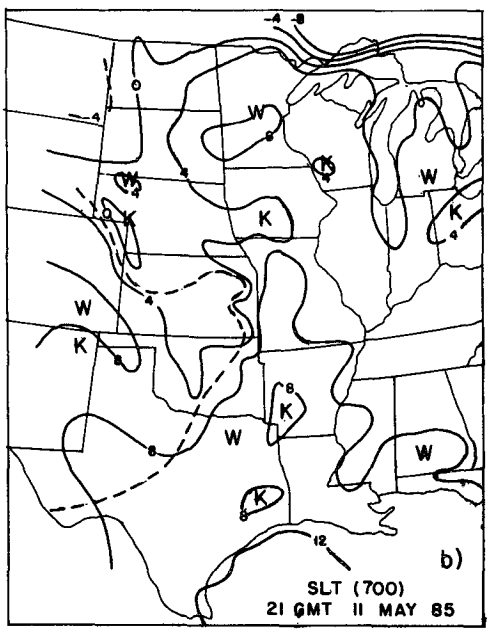

FIG. 12. As in Fig. 11 but for 2100 GMT.

of cold air at 700 and 500 mb, just north of the maximum west-southwesterlies, extended rapidly eastward to produce 12-h cooling up to 7°C in the layer from 700 to 500 mb in eastern Nebraska where we have seen the sudden development of a severe convective system (Figs. 10–11).

In the SLI(850) patterns (Figs. 13a and 14a), stability is seen in a long strip extending from northeastern Texas to the Great Lakes. It seems likely that this was associated with the preceding convective line discussed earlier and with cooling over the Great Lakes. The eastern and southwestern portions of the map showed instability, due probably to heating during the morning, but the former region was evidently too dry to produce deep cumulus convection (cf. Figs. 9a and 10a). A region of slight instability extending northward from eastern Kansas and western Missouri at 1800 GMT was interrupted 3 h later by the hail-bearing convective

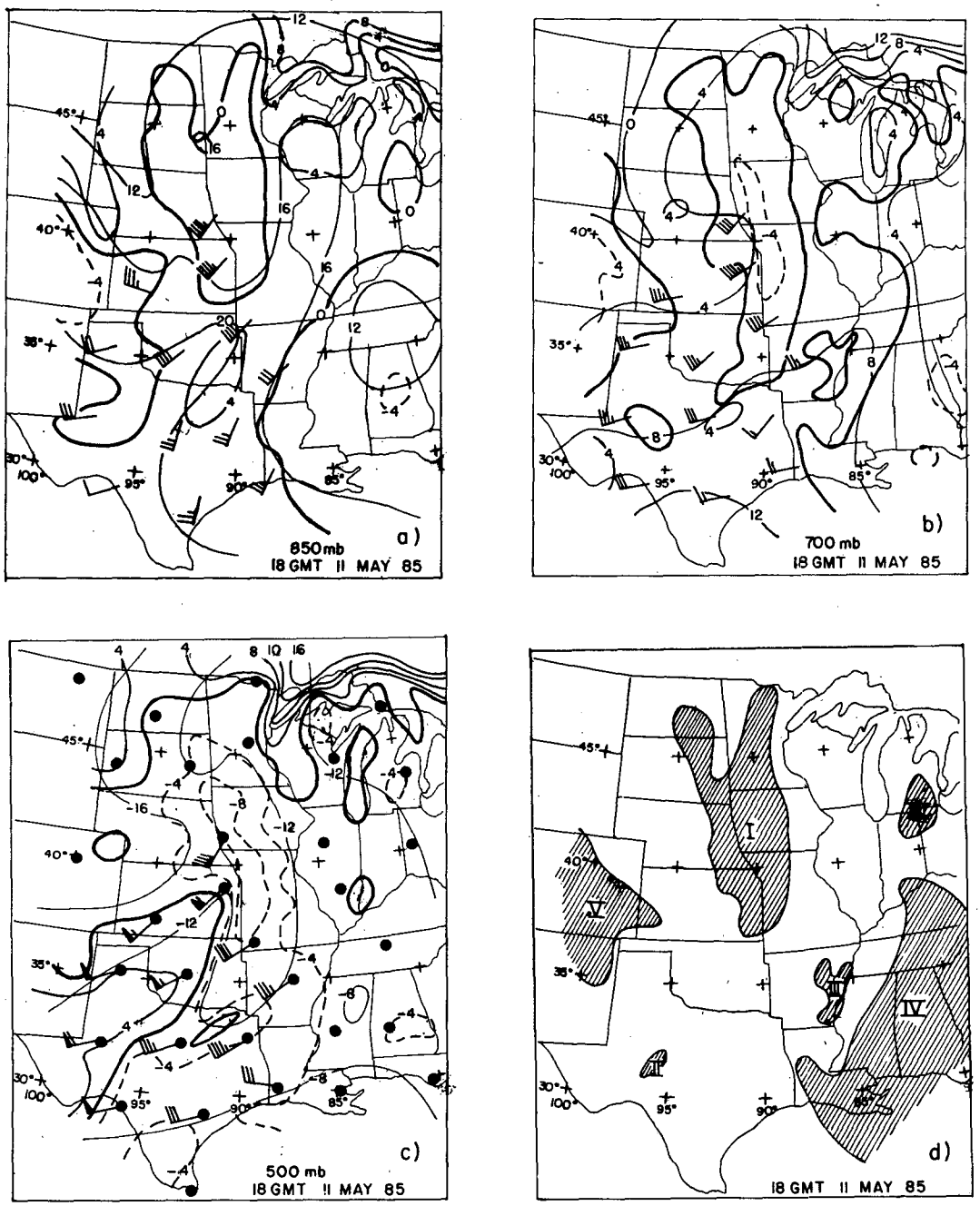

FIG. 13. For 1800 GMT 11 May 1985, and for (a) 850 mb, (b) 700 mb and (c) 500 mb, thin solid lines show ambient temperature field. Field of SLI shown by heavier solid (positive), heavier dashed (negative) and heaviest (zero) lines. All isopleths at intervals of 4°C. Part (d) shows hatching for areas in which SLI is negative at all three levels. Roman numerals refer to discussion in text.

system producing the first swath of severe events, described above.

Lifting of the surface air to 700 mb produced broadly similar patterns, although some differences in position are evident in Figs. 13b and 14b. The instability in the region northward from the Kansas–Missouri border was more intense, as a 4°C excess was indicated in SLI(700), broken at 2100 GMT by the severe storms in Iowa.

The fields of SLI(500), Figs. 13c and 14c, showed distinct differences. Most of the eastern half of the map area was unstable (except for strong stability seen in

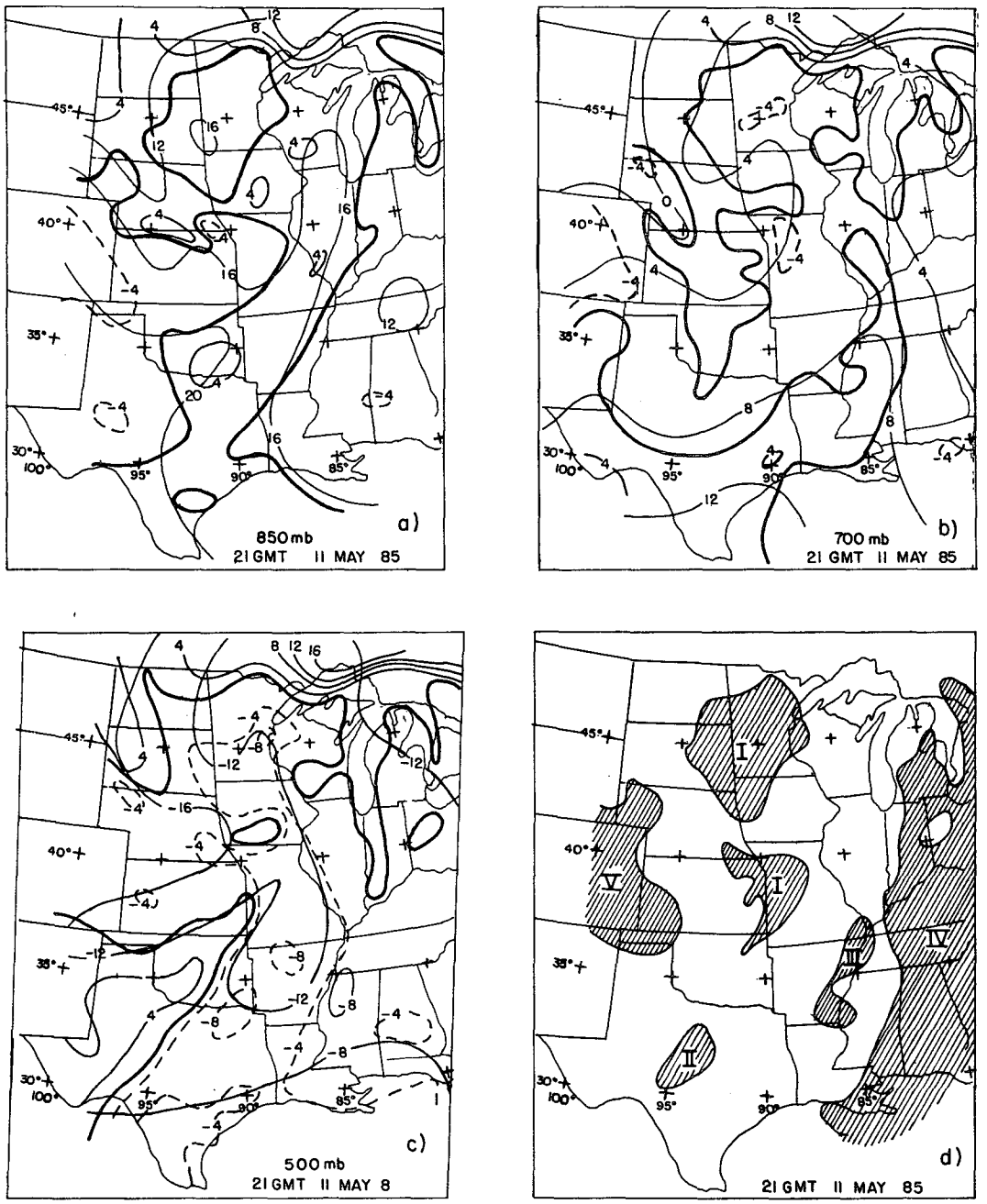

FIG. 14. As in Fig. 13 but for 2100 GMT.

all SLI-fields north of the Great Lakes and north of a frontal convergence line extending eastward from the South Dakota low). In the southwestern part of the map much of the instability seen for lower lifting levels was replaced by prominent stability, as relatively warm ambient temperatures at 500 mb overlay dry surface air. Along the confluence line between southerlies and southwesterlies (Figs. 9b and 10b), at the western edge of the major region of instability, SLI(500)-values of −8°C and lower were found from the Kansas–Missouri border north-northwestward to southeastern South Dakota at 1800 GMT. This region was broken and weakened by the Iowa storms by 2100 GMT, but by this time surface heating and moistening in northeastern Texas and western Arkansas had produced comparable values there.

Most of the region of unstable SLI(500) failed to produce deep convection. Some insight into the reasons why not can be obtained by superposition of the unstable regions for all three levels of lift, as seen in Figs. 13d and 14d. Five regions are seen, in which the potential instability represented by SLI(500) is not inhibited by positive values of SLI(850) or SLI(700), as discussed by Colby (1984).

Region I displayed the greatest instability and contained almost all the severe events reported between 1800 and 2100 GMT (Fig. 8). Similar instances of coincidence of severe convection and minimum SLT have been described by Hales and Doswell (1982).

Region II, a small area of large instability along the confluence line between southerlies and westerlies (Figs. 9b and 10b), was sandwiched, as in the case described by Colby (1980), between warm moist surface air to the southeast capped by a lid (Carlson et al., 1983) of dry air with distinctly higher potential temperature and air to the northwest with no such restriction, but with insufficient moisture to produce deep convection. Satellite and radar imagery showed the development of a line of detached cumulonimbus in the eastern portion of this region between 1800 and 2100 GMT, subsequently associated with a few severe events (Fig. 8).

Region III, in eastern Arkansas, lay just east of the strip of positive SLI for the 850 mb- and 700-mb levels associated with the earlier convection and was the site of renewed nonsevere convection during the period of study. The instability was not large.

Region IV, along the eastern edge of the map area, was associated with modest instability and widespread deep convection, but with little organization and no severe events reported.

Region V, in the eastern central Rockies with some extension into the high plains, was unstable but simply too dry to produce more than altocumulus castellanus (Figs. 9a and 10a), in this case evidently rooted in the deep surface boundary layer.

It is noteworthy that all reports of tornadoes or severe thunderstorm activity came from regions where SLI(500) was −4°C or lower, in agreement with Means' (1952) comment.

The details and strong gradients in the SLI fields, in Figs. 13 and 14, could not have been obtained in analyses based on stations as widely spaced as those of the routine rawinsonde network, even if soundings were taken at optimum times of day. Granted that in basing these fields on analyses of the ambient temperature fields at upper levels that do not contain comparable detail, there is the tacit assumption that the detail is much larger in the surface boundary layer than above. We feel that this assumption is not unreasonable, since transfers of heat and moisture from the land surface are probably patterned in a more detailed way than are the processes (aside from frontogenetical ones) that shape the temperature field in the free atmosphere.

The surface observational network is not an infallible source of detail, however. In numerous instances, especially near military bases or in large metropolitan areas, differences of 2°–4°C in SLT(500) at very closely spaced positions present a puzzle for analysis. They appear to result from differences in observations of surface dewpoint, some of which may well be in error. Ideally, one should keep track of such discrepancies and try to decide which of such observations to correct or ignore. We have not done that.

We have made no attempt to assess the importance of kinematic aspects of this situation, in particular the possible influence of jet streaks (Uccellini and Johnson, 1979) and of wind shear in general on the development of convection, a subject whose importance was recognized long ago (Fawbush et al., 1951) and whose relationship to rotating quasi-steady thunderstorms has been recently analyzed by Lilly (1986). We note only that Region IV was characterized by light winds accompanying disorganized convection and that most of the severe convection in Region I occurred just ahead of a moderately strong west-southwesterly jet (Fig. 11c).

5. Concluding summary

We have argued for the usefulness of the surface-lifted-temperature (SLI) introduced by Means (1952) in the prediction of deep convection in middle latitudes. This quantity is obtained by subtracting the temperature of an adiabatically lifted surface air parcel (SLT) from the ambient temperature at the level to which the parcel is lifted.

Examination of the thermodynamical background of the lifting process shows that for a typical cold-air sample, the sensitivity of the SLT at 500 mb, SLT(500), is greater for a given increment of surface temperature than for the same increment of surface dewpoint. The opposite is the case for a typical sample of warm humid air. The reason for this difference is that despite the much larger increment of surface equivalent-potential temperature, θ_e, for the warmer sample, most of this increase goes into raising the saturation mixing ratio of the lifted parcel, q_s, than into raising its temperature. For the colder sample, the effects of water vapor are relatively inconsequential.

Nomograms are presented for obtaining SLT(850), SLT(700) and SLT(500) as a function of surface temperature and dewpoint, for a station pressure of 950 mb. Corrections for departure of station pressure from this value are included, and are separately mapped for SLT(500) over the contiguous United States. A separate nomogram for SLT(500), for a station pressure of 1000 mb, is included, for use over the sea.

As an example (although based on SLIs produced by computer), we presented the case of 11 May 1985

in the central United States. Deep convection was well related to areas of substantial negative SLI(500) with no positive values of SLI(850) or SLI(700) in the air column. Most severe convective events occurred in regions with substantial vertical wind shear.

Acknowledgments. The author is indebted to Bob Maddox, NOAA/NSSL, and to Joe Schaefer, NWS Central Region, for calling his attention to the existence of Means's memorandum, for providing a replacement of the mislaid original copy, and for discussing present practice at NSSFC. He is also grateful to Kerry Emanuel, MIT, for stimulating disputation, and to the Center for Meteorology and Physical Oceanography for provision of data and facilities. Thanks are due to Isabelle Kole for drafting of illustrations. This research was supported by the National Science Foundation under

REFERENCES

Barnes, S., 1970: Some aspects of a severe right-moving thunderstorm deduced from mesonetwork rawinsonde observations. *J. Atmos. Sci.*, **27**, 634–648.

Carlson, T. N., S. G. Benjamin, G. S. Forbes and Y.-F. Li, 1983: Elevated mixed layers in the regional severe storm environment: Conceptual model and case studies. *Mon. Wea. Rev.*, **111**, 1453–1473.

Colby, F. P. Jr., 1980: The role of convective instability in an Oklahoma squall line. *J. Atmos. Sci.*, **37**, 2113–2119.

——, 1984: Convective inhibition as a predictor of convection during AVE-SESAME II. *Mon. Wea. Rev.*, **112**, 2239–2252.

Darkow, G. L., and R. L. Livingston, 1975: Hourly surface static energy analysis as a delineator of thunderstorm outflow areas. *Mon. Wea. Rev.*, **103**, 817–822.

Drogemeier, K. K., and R. B. Wilhelmson, 1985: Three-dimensional numerical modeling of convection produced by interacting thunderstorm outflows. Part I: Control simulation and low-level moisture variations. *J. Atmos. Sci.*, **42**, 2381–2403.

Fawbush, E. J., R. C. Miller and L. G. Starrett, 1951: An empirical method of forecasting tornado development. *Bull. Amer. Meteor. Soc.*, **32**, 1–9.

Galway, J. G., 1956: The lifted index as a predictor of latent instability. *Bull. Amer. Meteor. Soc.*, **37**, 528–529.

Hales, J. E., Jr., and C. A. Doswell III, 1982: High resolution diagnosis of instability using hourly surface lifted parcel temperatures. *Preprints 12th Conf. on Severe Local Storms,* San Antonio, Amer. Meteor. Soc., 324 pp.

Lilly, D. K., 1986: The structure, energetics and propagation of rotating convective storms. Part I: Energy exchange with the mean flow. *J. Atmos. Sci.*, **43**, 113–125.

Means, L. L., 1952: Stability index computation graph for surface data. Attachment to U.S. Department of Commerce Weather Bureau Multiple Address Letter No. 112-52. [Copy can be obtained from F. Sanders, 9 Flint Street, Marblehead, MA 01945.]

Mostek, A., L. W. Uccellini, R. A. Petersen and D. Chesters, 1986: Assessment of VAS soundings in the analysis of a preconvective environment. *Mon. Wea. Rev.*, **114**, 62–87.

Showalter, A. K., 1953: A stability index for thunderstorm forecasting. *Bull. Amer. Meteor. Soc.*, **34**, 250–252.

Uccellini, L. W., and D. R. Johnson, 1979: The coupling of upper and lower tropospheric jet streaks and implications for the development of severe convective storms. *Mon. Wea. Rev.*, **107**, 682–703.

U.S. Weather Bureau, Staff Members, National Severe Storms Project, 1963: Environmental and thunderstorm structures as shown by the National Severe Storms Project in Spring 1960 and 1961. *Mon. Wea. Rev.*, **91**, 271–292.

U.S. Dept. of Commerce, 1985: *Storm Data,* 27, No. 5.